Transactions on Machine Intelligence 8(4) (2025) 259–268

ISSN Online: 2821-1693

Transactions on Machine Intelligence

Journal Homepage: https://tmachineintelligence.ir/index.php/TMI



Artificial Intelligence for Matte Grade Prediction in Copper Flash Smelting

H. Ghayoumi Zadeh[1*]

[1] Associate Professor, Department of Electrical Engineering, Vali-e-Asr University of Rafsanjan, Rafsanjan, Iran

ARTICLE INFO

Article History:
Received 8 August 2025
Received in revised form 28 November 2025
Accepted 27 December 2025
Available online 30 December 2025

Keywords:
Copper Flash Smelting, Matte Grade, Ridge Regression, Soft Sensor, Rolling-Origin Validation

ABSTRACT

The copper content of matte is a critical performance indicator in flash smelting; however, laboratory assay results are typically unavailable until after tapping. This study evaluated two soft-sensing approaches for estimating matte copper grade at the time of tapping using industrial records comprising 8,653 matte taps, 9,012 slag taps, and 7,032 hourly process observations. The first approach employed ridge autoregression with exogenous inputs derived from process measurements and lagged assay results. The second adapted a stoichiometric oxygen-balance model using recent assay information. Performance was evaluated across five rolling-origin test periods covering 4,533 taps over 162 days, assuming a two-hour assay delay. Ridge autoregression achieved the lowest pooled mean absolute error (MAE) of 1.519 percentage points of copper (95% confidence interval: 1.389–1.626), significantly outperforming persistence, which achieved an MAE of 1.592 percentage points ($p = 0.0019$). Incorporating assay feedback reduced the mass-balance model error substantially, from 4.694 to 1.599 percentage points. The recorded target generated by the commercial advisory system showed a mean absolute deviation of 1.813 percentage points from the measured matte grade. Overall, the findings demonstrate the value of a compact data-driven predictor and show that incorporating updated assay information can substantially improve mass-balance estimates. Further validation using actual assay release times and strictly forward-looking feed imputation is required to establish real-time operational performance.

1. INTRODUCTION

1.1. Matte Grade and the Measurement Delay

Flash smelting oxidises a dry sulphide concentrate in a suspension of oxygen-enriched gas. The reaction products enter the settler, where the copper-bearing matte separates from iron-silicate slag. Matte grade is the copper mass fraction in the matte. It describes the composition sent to downstream converting and depends on how iron and sulphur partition between matte, slag and gas [1]. The concentrate blend and oxygen supplied per tonne of feed therefore matter to grade estimation, and two taps with similar oxygen flows may represent different operating conditions if the feed rate or chemistry changes.

* Corresponding author: h.ghayoumizadeh@vru.ac.ir
Associate Professor, Department of Electrical Engineering, Vali-e-Asr University of Rafsanjan, Rafsanjan, Iran

http://dx.doi.org/10.22034/tmi.2025.256841

© 2025 by the authors. Licensee T.M.I, Tehran, Iran. This article is an open access article distributed under the terms and conditions of the Creative Commons Attribution (CC-BY) license (http://creativecommons.org/licenses/by/4.0/).

Furnace inputs and tap assays are observed on different schedules. Process measurements are logged hourly in the present archive, blend assays are attached by shift, and matte is sampled at irregular tap times. In addition, sampling and laboratory analysis separate the tap timestamp from the time when its copper result is available. The estimation task is to infer the grade of the tap at the time of tapping, before its assay becomes available. The most recent recorded assay is useful only if it would already have been released by that time.

There is also a physical timing issue. The feed and oxygen readings nearest a tap need not reflect all the material contributing to its composition. Settler simulations indicate that flow patterns vary with tapping configuration, while droplet-scale simulations show that settling is influenced by coalescence and reaction [2][3]. These studies motivate accounting for process history. In the present study, a single fitted first-order filter summarises that history. Its fitted time constant represents smoothing in the archived signals.

1.2. Previous Work on Matte Grade Prediction

Gui et al. combined a mechanistic model and a fuzzy neural network to estimate matte grade in copper flash smelting [4]. Yang et al. combined a reaction-based model with a neural predictor and adapted their relative contributions through a fuzzy coordinator [5]. Liu et al. used dynamic species balances and equilibrium relations to represent the flash furnace and validated the approach against plant data [6]. These studies show how operating data and metallurgical balances can support prediction. In this work, the adaptation is confined to an effective oxygen factor in the mass balance, which can be inferred directly from each eligible historical assay.

Recent studies have focused on how to represent the timing of process variables. Zhang et al. combined temporal convolutions and attention to extract patterns from multivariate smelting signals [7]. Zou et al. used a knowledge-guided encoder–decoder with variable weighting and temporal decay to represent the relevance of process measurements over time [8]. In oxygen-rich side-blown bath smelting, He et al. paired lagged features with local Gaussian-process regression and evaluated updates based on sliding windows and just-in-time learning [9]. That study concerns a different furnace design. It illustrates the wider importance of asynchronous inputs and updating when operating conditions change.

The studies provide alternatives for representing process history, but their reported errors are tied to their respective furnaces, input availability, validation periods and error definitions. The practical question for this archive is whether a compact model adds predictive information beyond already available assays, and how much of the static mass-balance error is removed by feedback. These questions require all comparisons to use the same taps, with a common rule for assay availability.

1.3. Study Objectives and Evaluation Design

We compare a ridge autoregression, a feedback-adjusted mass balance and three prediction baselines on a common chronological test set. Persistence and an exponentially weighted average establish how much can be predicted from recent assays alone. The static mass balance isolates the change associated with updating its oxygen factor, while the plant advisor target serves as a reference for how closely the archived grades followed the recorded target. The key outcomes are pooled prediction error, variability across chronological test blocks and agreement at selected absolute-error thresholds.

We use repeated chronological holdouts to examine the stability of the comparisons over the observed operating period. Multiple holdouts allow performance to be examined across changing conditions [10][11]. The two-hour assay assumption governs which matte results enter feedback and lagged features. Other information pathways, including the use of daily blend means for some missing shifts, are considered separately when interpreting what the retrospective results imply for live use.

2. INDUSTRIAL DATA

The records cover an Outokumpu-type copper flash furnace from 21 April 2021 to 21 March 2022. The archive contains 293 daily logs, 7,032 hourly process rows, 8,653 matte tap records and 9,012 slag tap records. Table 1 summarises selected variables using the valid observations for each variable. Plant logs capture concentrate and dust

feed, gas flows and advisory values. Tap records provide copper assays and temperature, while slag iron and silica assays are used to calibrate flux utilisation.

The data pipeline screened out-of-range measurements, including 15 hourly feed readings and 10 matte temperatures. Feed composition was computed as the blend-share-weighted mean of valid concentrate assays for each shift. Where a shift blend was missing, the code used the mean of available blends from that day, followed by forward filling and an initial fill with the earliest available blend. Matte taps were matched to the most recent filtered process record within three hours. For evaluation, matte assays were assumed to be available two hours after each tap.

Table 1. Descriptive statistics for selected furnace and tap measurements.

Variable	Unit	Valid records	Mean	Standard deviation	Median	25th–75th percentile
Logged feed rate	t/h	6,469	111.8	8.5	115.0	105.0–119.0
Flue dust recycle	t/h	6,472	8.25	0.95	8.30	7.70–8.90
Process air flow	Nm³/h	6,415	23,711	2,591	23,666	21,876–25,298
Advisor oxygen enrichment	%	6,418	46.7	1.9	46.8	45.5–48.0
Matte copper grade	wt%	8,636	49.48	2.20	49.59	48.20–50.86
Matte iron	wt%	8,637	19.64	2.05	19.48	18.28–20.87
Matte sulphur	wt%	8,642	19.65	1.03	19.56	19.04–20.27
Matte temperature	°C	8,547	1,238	11	1,238	1,230–1,245
Slag iron-to-silica ratio	–	8,776	1.38	0.15	1.37	1.28–1.48
Slag copper	wt%	8,872	1.12	0.42	1.06	0.90–1.26
Slag temperature	°C	8,849	1,298	10	1,298	1,292–1,303

The archive record count and the number used to score the models serve different purposes. The archive includes taps with missing values and periods used for initial calibration. The comparison uses only taps in the test periods for which all methods produced an estimate. The descriptive statistics in Table 1 use available values for each variable, so their sample sizes vary across rows.

3. METHODS

3.1. Dynamic Mass Balance

The model partitions copper, iron and sulphur between matte, slag and gas. The feed vector also includes silica and alumina. For candidate grade g in weight percent copper, the fixed matte composition relations in the implementation are Fe = 50.55 − 0.6248g and S = 23.99 − 0.0876g, both in weight percent. Slag copper is set to 1.10 wt%, and the model assigns 15% of slag iron to magnetite. Each fold estimates silica delivered per tonne of flux using training-period slag iron-to-silica ratios. The fixed empirical constants are inherited from the plant model.

The partition allocates matte sulphur to copper and iron sulphides. Sulphur outside matte is assigned to sulphur dioxide. Equation (1) expresses the stoichiometric oxygen requirement, with all molar rates in kmol/h. The magnetite term counts moles of iron in magnetite, including the matte and slag contributions.

$$n(O_2) = n(SO_2) + \tfrac{1}{2}n(FeO) + \tfrac{2}{3}n(\text{Fe in magnetite}) \quad (1)$$

The molar requirement is converted to normal cubic metres per hour using 22.414 Nm³/kmol. Available oxygen is calculated from process and distribution air and process and lance oxygen, with a deduction for natural gas at the burner. An exponentially weighted first-order filter represents the smoothing effect of the settler on process inputs. At irregular intervals, the weight assigned to the new measurement is $1 - \exp(-\Delta t/\tau)$, where τ is the fitted time constant. The filter restarts after gaps longer than eight hours.

For each historical matte assay, the observed oxygen factor η is the ratio of stoichiometric oxygen implied by the measured grade to estimated available oxygen. The static model uses the training median. The adaptive model

averages the factors from assays within a fitted window ending two hours before the current tap. It falls back to the latest eligible factor or the training median. For either model, bisection on 25–78 wt% Cu finds the grade at which stoichiometric oxygen matches available oxygen multiplied by the selected factor. Fig. 1 shows the process inputs and feedback shared by the predictors. The grade benchmark uses the oxygen balance. Heat-loss calibration belongs to the wider advisory model.

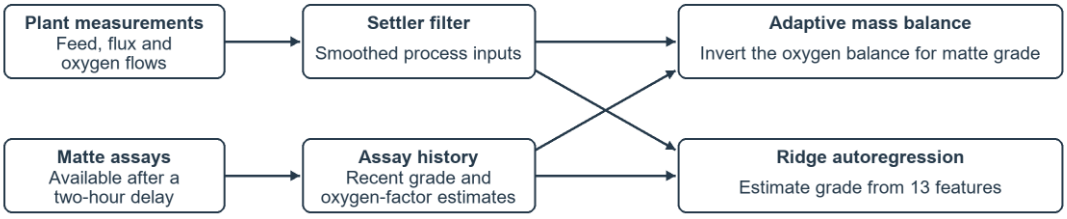


Fig. 1. Process and assay inputs for the two evaluated grade predictors.

The oxygen factor is estimated by comparing the stoichiometric requirement implied by a tap assay with the available oxygen inferred from logged flows. In the static formulation a single median scales the available oxygen throughout a test block. In the adaptive formulation the scaling changes as new assay results become eligible. As a result, differences between these variants reflect the use of delayed observations within the same inversion, while the source of any individual oxygen discrepancy remains unresolved.

3.2. Ridge Autoregression and Baselines

The ridge autoregression with exogenous inputs (ARX) uses 13 features. Four describe available assay history (the latest eligible grade and means over 2, 6 and 24 hours). The remaining nine are the filtered oxygen coefficient (available oxygen per tonne of feed), its change relative to the lagged two-hour average, oxygen enrichment, feed rate, concentrate copper, iron and sulphur percentages, flux percentage and the lagged oxygen factor. The model standardises each predictor using training means and standard deviations and fits a linear regression with an L2 penalty on the coefficients [12]. The penalty is selected from 0.1, 1, 10 and 100 using the final 20% of each training period in chronological order. The model is then refitted on the full training period.

For a tap at time t, the 2-hour assay mean draws on tap times from t − 4 hours to t − 2 hours. The 6- and 24-hour means end at the same availability cut-off. If the window has no valid value, the implementation uses the most recent eligible assay. This alignment prevents using the current tap result in its own prediction. The oxygen coefficient and the lagged oxygen factor represent different quantities. The coefficient measures supply per tonne of feed, and the factor represents disagreement between logged supply and the requirement inferred from earlier assays.

The persistence baseline is a mean of recent eligible assays. The exponentially weighted moving average (EWMA) assigns greater weight to newer eligible assays. Their window and half-life are selected on training data. The recorded Outotec Advisor series is a grade target. Its error measures deviation of actual grade from the target and provides an operational reference. The implementation passes the target series through the same first-order filter before comparison.

3.3. Rolling-Origin Evaluation

Five expanding training windows end at 50%, 60%, 70%, 80% and 90% of the time span, and each following block is held out in turn. Within each training window, the settler time constant (2, 4, 6, 8, 12, 16, 24, 36 or 48 hours) and the oxygen feedback window (1, 2, 4 or 6 hours) are chosen by training mean absolute error (MAE). Persistence windows of 1, 2, 4, 6 and 12 hours and EWMA half-lives of 1, 2, 4, 8 and 16 hours are also compared on the training portion. The test set contains 4,533 taps across 162 days with estimates from all methods.

Errors are expressed in percentage points of copper. Bias is estimate minus assay, averaged across taps. Pooled MAE and root mean square error (RMSE) give equal weight to each tap. Percentile confidence intervals use 2,000 moving-block bootstrap resamples with blocks of seven observed days [13]. The Diebold–Mariano comparisons use

daily mean differences in absolute error and Newey–West variance estimates with seven lags [14][15]. These tests weight each observed day equally. The reported pairwise p-values are two-sided and unadjusted.

The expanding-window comparison retains earlier operating records at each new origin. During each test period the model can use an earlier test tap once that tap satisfies the assumed assay delay. This matches a monitoring task in which observed grades become available progressively. Model calibration is updated at the next fold origin. The paired comparisons use the same observed tap outcomes, which makes it possible to distinguish differences in model error from differences in the composition of the scoring sample.

4. RESULTS AND DISCUSSION

4.1. Predictive Accuracy

Ridge ARX achieved the lowest pooled MAE (1.519) and RMSE (1.989) of the methods evaluated (Table 2). Its MAE was 0.073 percentage points lower than persistence, with a paired 95% bootstrap interval of −0.105 to −0.035 for the difference and a daily Diebold–Mariano p-value of 0.0019. The daily absolute-error comparison also favoured ridge ARX over the adaptive balance ($p = 0.0234$). Fig. 2 compares measured and estimated grades for the two predictors.

Table 2. Pooled out-of-sample errors for 4,533 matte taps. All values are in percentage points of copper.

Method	MAE	95% interval for MAE	RMSE	Bias
Ridge ARX	1.519	1.389 to 1.626	1.989	+0.126
EWMA	1.570	1.435 to 1.679	2.168	-0.020
Persistence	1.592	1.461 to 1.693	2.202	-0.021
Adaptive balance	1.599	1.471 to 1.696	2.243	-0.030
Advisor target	1.813	1.646 to 1.965	2.325	-0.146
Static balance	4.694	3.437 to 6.065	6.195	+2.888

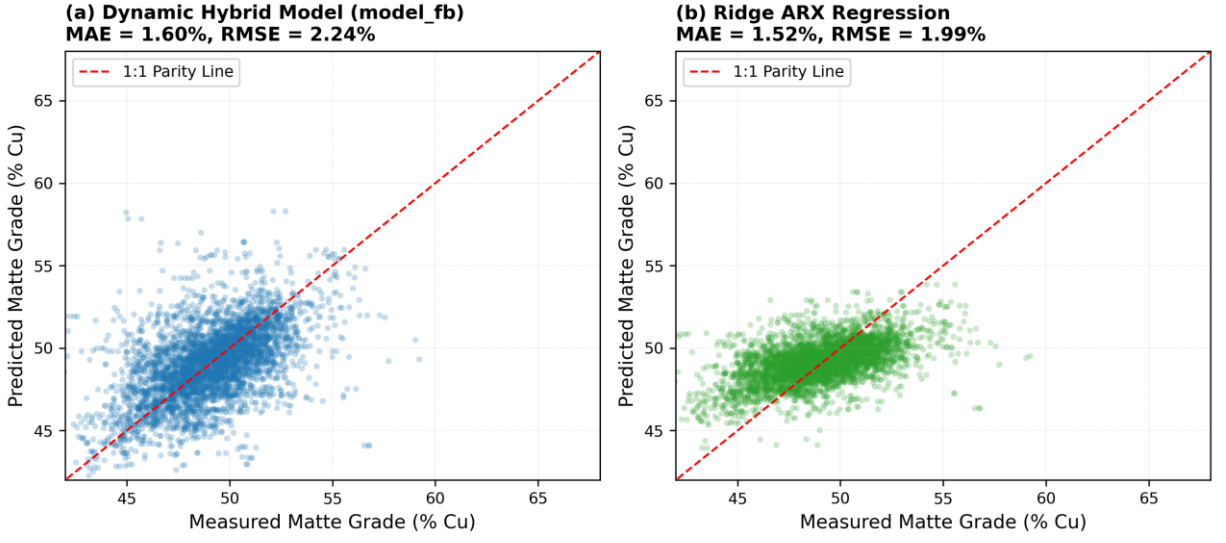


Fig. 2. Measured and predicted matte grade for the adaptive balance and ridge ARX. The panels show the central grade range. Reported metrics use all evaluation taps.

The adaptive balance reduced MAE from 4.694 for the static balance to 1.599. The advisor target had an MAE of 1.813 (adaptive balance versus target, $p = 0.0127$). Persistence and EWMA had similar or lower pooled MAEs than the adaptive balance, and their daily loss comparisons with the adaptive balance yielded $p = 0.5261$ and $p = 0.3766$, respectively. The benefit of the feedback update is clearest within the mass-balance model family.

4.2. Performance Across Test Periods

Ridge ARX had the lowest MAE in each test block (Table 3). The adaptive balance was closer to the measured grade than the advisor target in four of the five blocks. The static balance worsened from an MAE of 2.76 in the first block to 9.31 in the last. The 48-hour settler time constant and the two-hour feedback window were selected in all five folds. Since 48 hours was the largest value tested, it is best interpreted as an empirical smoothing timescale.

Table 3. Mean absolute error by test block, in percentage points of copper.

Fold	Test end	Taps	Ridge ARX	EWMA	Persistence	Adaptive balance	Advisor target	Static balance
1	2021-11-07	916	1.31	1.33	1.38	1.46	1.42	2.76
2	2021-12-11	953	1.33	1.38	1.43	1.44	1.57	2.88
3	2022-01-13	815	1.58	1.64	1.63	1.63	1.97	2.98
4	2022-02-15	831	1.54	1.60	1.61	1.57	2.06	4.93
5	2022-03-21	1,018	1.82	1.88	1.89	1.87	2.06	9.31

The fold comparison also shows why the pooled ranking should be read alongside the chronology. In the first test block the adaptive balance had an MAE of 1.46, compared with 1.42 for the advisor target and 1.38 for persistence. In the final block the adaptive balance had an MAE of 1.87, close to persistence at 1.89, while the static balance reached 9.31. The larger late-period gap between the static and adaptive balances shows where the feedback mattered most in this archive. The results do not isolate an individual plant change responsible for the static model’s increased error.

4.3. Oxygen Balance and Measurement Variability

In the plant-model calibration, the training median oxygen factor was 1.186. The oxygen-balance discrepancy, estimated as $(\eta - 1)$ times the median estimated available oxygen flow, was approximately 3,437 Nm³/h. The median logged oxygen equivalent of the sulphatising streams was approximately 2,340 Nm³/h, or 68% of that discrepancy. This ratio compares logged supply with a model-derived difference. The data do not identify actual oxygen consumption by dust or independently attribute the residual to individual mechanisms. Fig. 3 shows the full-record factor distribution (median 1.175), along with the tap-grade series and rolling errors.

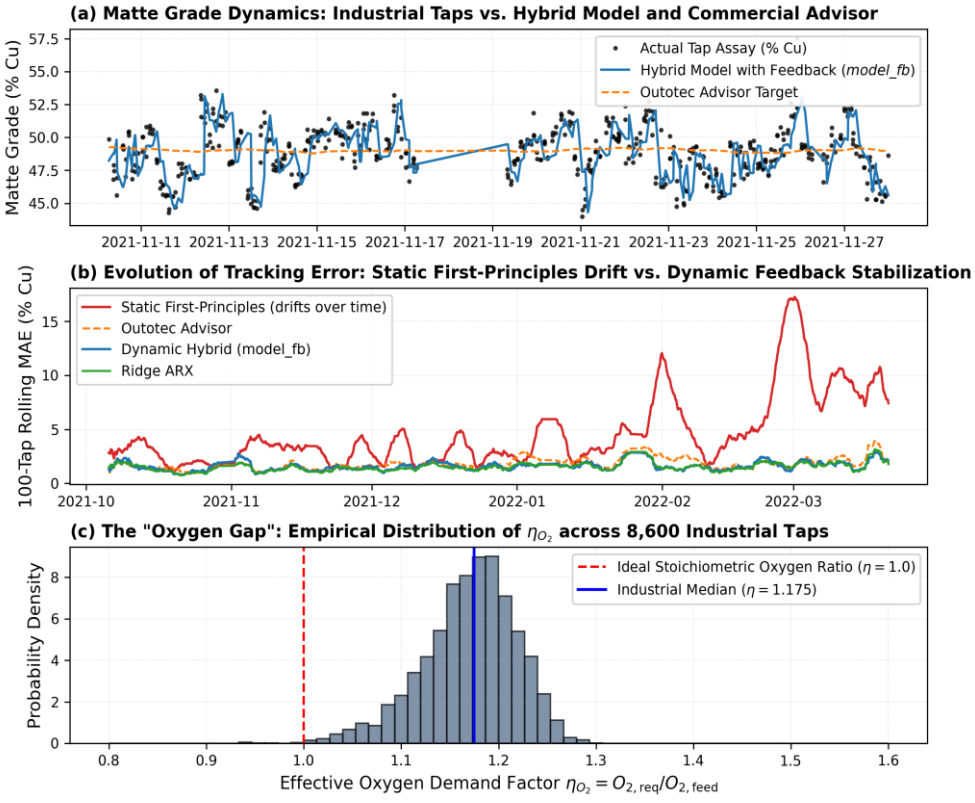


Fig. 3. Example tap-grade series, 100-tap rolling mean absolute error and distribution of the observed oxygen factor. The histogram median describes the full modelled record.

The mean absolute assay difference for 2,639 successive evaluation tap pairs no more than 20 minutes apart was 0.714 percentage points of copper. This difference includes short-term process variation and sampling or analytical variability. It describes the observed repeatability of neighbouring tap assays and does not establish a lower bound on prediction error.

Dust sampling at an industrial flash-smelting waste heat boiler has shown that collected species can differ from thermodynamic equilibrium predictions [16]. For the present dataset, logged oxygen delivered to sulphatising streams therefore provides context for the model discrepancy. It does not determine how much oxygen reacted with the dust. Quantifying that allocation would require measured flows and compositions for the streams involved and independent measurements of the dust reactions.

4.4. Limitations and Operational Interpretation

This is a retrospective evaluation at one plant under an assumed assay delay. Same-day blend imputation can use information from later shifts, and actual laboratory release timestamps were unavailable in the evaluation files. Some empirical constants were inherited from the plant model. Their calibration provenance should be verified before treating all hold-outs as fully independent. A prospective replay using recorded release times, forward-only imputation and fold-specific calibration would establish the magnitude of these effects.

The commercial target was included because it is part of the operating record. A small deviation between the target and the assay can reflect target selection, operator response and furnace behaviour. An error comparison with this series should therefore be interpreted as a comparison with the recorded operating target. Establishing whether the soft sensor improves control requires a separate study in which its estimates inform decisions and the consequences are measured.

A follow-up validation would track when blend information, process measurements and assays actually enter the operator's system, then replay those records in that order. Stratifying errors by feed blend and by time since the last available assay would show where the model adds the most information. A feature-ablation study would also be needed to quantify how much of the ridge model's gain comes from oxygen and feed variables beyond the assay history.

The results concern the estimation of grade at tapping. The models were assessed against archived assays and were not used to change plant controls. Prediction error alone cannot quantify the effect of deploying either model on oxygen consumption, slag losses or furnace stability.

4.5. Frequency and Magnitude of Larger Errors

Table 4 reports additional error summaries computed from the 4,533 saved out-of-sample predictions. The two thresholds describe how often the absolute error stays within a given distance of the assay. The 90th percentile describes the magnitude at the upper end of the error distribution. These thresholds are descriptive and are not plant acceptance limits.

Table 4. Error thresholds and 90th-percentile absolute error on the common test set.

Method	Error ≤ 1 point (%)	Error ≤ 2 points (%)	90th percentile (points)
Ridge ARX	42.4	72.6	3.22
EWMA	45.1	71.7	3.42
Persistence	45.4	71.0	3.52
Adaptive balance	45.3	71.2	3.47
Advisor target	35.3	63.5	3.66
Static balance	14.3	28.2	10.40

Ridge autoregression had the highest share of estimates within two percentage points (72.6%) and the lowest 90th-percentile absolute error (3.22 points). At the one-point threshold, persistence had a higher share of estimates within the threshold, 45.4% compared with 42.4% for ridge autoregression. The lower mean error of ridge autoregression therefore did not translate into more estimates within every tolerance. This pattern is relevant when the cost of a larger error differs from the cost of a smaller one.

5. CONCLUSIONS

In five chronological test periods at an industrial copper flash furnace, ridge ARX produced the lowest grade prediction error among the evaluated methods, with an MAE of 1.519 percentage points of copper. Assay feedback reduced the MAE of the static mass balance from 4.694 to 1.599. Ridge ARX offers a compact predictor for this dataset, and the adaptive balance provides an interpretable estimate tied to oxygen and feed. The retrospective design and availability of input data at prediction time limit claims about live performance.

Acknowledgements

The authors thank the smelter operations and metallurgy teams for providing the plant records and supporting the study.

Declaration

The authors acknowledge the use of ChatGPT as a language-support tool to improve the clarity, readability, and academic presentation of the manuscript. The authors take full responsibility for the scientific content, methodology, analyses, results, and conclusions presented in this study and have ensured the originality and integrity of the work.

Transparency Statement

The industrial process data used in this study are subject to confidentiality and proprietary restrictions. Therefore, the raw data are not publicly available. However, data or additional methodological information may be made available by the corresponding author upon reasonable request, subject to the approval of the data owner and applicable confidentiality requirements.

Declaration of Interest

The authors declare that they have no competing interests.

Funding

This research received no specific grant from any funding agency in the public, commercial, or not-for-profit sectors.

REFERENCES

[1] Taskinen, P., Jokilaakso, A., Lindberg, D., & Xia, J. (2020). Modelling copper smelting–the flash smelting plant, process and equipment. *Mineral Processing and Extractive Metallurgy, 129*(2), 207–220. https://doi.org/10.1080/25726641.2019.1688904

[2] Zhou, J., Chen, Z., Zhou, P., Yu, J.-P., & Liu, A.-M. *(2012). Numerical simulation of flow characteristics in settler of flash furnace. Transactions of Nonferrous Metals Society of China, 22*(6), 1517–1525. https://doi.org/10.1016/S1003-6326(11)61350-2

[3] Jylhä, J. P., & Jokilaakso, A. *(2023). CFD-DEM models for matte droplet settling in a flash smelting settler. Heliyon, 9*(11), e21570. https://doi.org/10.1016/j.heliyon.2023.e21570

[4] Gui, W.-H., Wang, L.-Y., Yang, C.-H., Xie, Y.-F., & Peng, X.-B. *(2007). Intelligent prediction model of matte grade in copper flash smelting process. Transactions of Nonferrous Metals Society of China, 17*(5), 1075–1081. https://doi.org/10.1016/S1003-6326(07)60228-3

[5] Yang, C.-H., Xie, M., Gui, W.-H., & Peng, X.-B. *(2008). A prediction model for matte grade in copper flash smelting process. Information and Control, 37*(1), 28–33. https://xk.sia.cn/en/article/id/11

[6] Liu, J.-H., Gui, W.-H., Xie, Y.-F., & Yang, C.-H. *(2014). Dynamic modeling of copper flash smelting process at a smelter in China. Applied Mathematical Modelling, 38*(7–8), 2206–2213. https://doi.org/10.1016/j.apm.2013.10.035

[7] Zhang, J., Li, Z., Wang, E., Yu, B., Li, J., & Ma, J. *(2024). A temporal network based on characterizing and extracting time series in copper smelting for predicting matte grade. Sensors, 24*(23), 7492. https://doi.org/10.3390/s24237492

[8] Zou, Z., Zhou, C., & Yang, C. *(2025). Knowledge-guided encoder-decoder network for soft sensor of copper matte grade in flash smelting process. Neurocomputing, 656*, 131485. https://doi.org/10.1016/j.neucom.2025.131485

[9] He, M. Q., Yu, G., Yang, C., & Han, L. *(2023). Dynamic soft sensor modeling of matte grade in copper oxygen-rich side blow bath smelting process. Measurement, 223*, 113792. https://doi.org/10.1016/j.measurement.2023.113792

[10] Cerqueira, V., Torgo, L., & Mozetič, I. *(2020). Evaluating time series forecasting models: An empirical study on performance estimation methods. Machine Learning, 109*(11), 1997–2028. https://doi.org/10.1007/s10994-020-05910-7

[11] Tashman, L. *J. (2000). Out-of-sample tests of forecasting accuracy: An analysis and review. International Journal of Forecasting, 16*(4), 437–450. https://doi.org/10.1016/S0169-2070(00)00065-0

[12] Hoerl, A. E., & Kennard, R. *W. (1970). Ridge regression: Biased estimation for nonorthogonal problems. Technometrics, 12*(1), 55–67. https://doi.org/10.1080/00401706.1970.10488634

[13] Künsch, H. *R. (1989). The jackknife and the bootstrap for general stationary observations. The Annals of Statistics, 17*(3), 1217–1241. https://doi.org/10.1214/aos/1176347265

[14] Diebold, F. X., & Mariano, R. *S. (1995). Comparing predictive accuracy. Journal of Business & Economic Statistics, 13*(3), 253–263. https://doi.org/10.1080/07350015.1995.10524599

[15] Newey, W. K., & West, K. D. (1987). A simple, positive semi-definite, heteroskedasticity and autocorrelation consistent covariance matrix. *Econometrica, 55*(3), 703–708. https://doi.org/10.2307/1913610

[16] Schmidt, A., Guy, B. M., Montenegro, V., Reuter, M., Charitos, A., Stelter, M., & Richter, A. *(2023). Flue dust reactions and sticking mechanisms in a copper flash smelting furnace waste heat boiler: A sampling study. Journal of Sustainable Metallurgy, 9*, 848–859. https://doi.org/10.1007/s40831-023-00691-4